Preconditioned Conjugate-Residual Solvers for Helmholtz Equations in Nonhydrostatic Models

WILLIAM C. SKAMAROCK, PIOTR K. SMOLARKIEWICZ, AND JOSEPH B. KLEMP

National Center for Atmospheric Research,* Boulder, Colorado

ABSTRACT

Numerical integration of the compressible nonhydrostatic equations using semi-implicit techniques is complicated by the need to solve a Helmholtz equation at each time step. The authors present an accurate and efficient technique for solving the Helmholtz equation using a conjugate-residual (CR) algorithm that is accelerated by ADI preconditioners. These preconditioned CR solvers possess four distinct advantages over most other solvers that have been used with the Helmholtz equations that arise in compressible nonhydrostatic semi-implicit atmospheric models: the preconditioned CR methods 1) can solve Helmholtz equations containing variable coefficients, alleviating the need to prescribe a reference state in order to simplify the elliptic problem; 2) transparently include the cross-derivative terms arising from terrain transformations; 3) are efficient and accurate for nonhydrostatic models used across a broad range of scales, from cloud scales to synoptic-global scales; and 4) are easy to formulate and program. These features of the CR solver allow semi-implicit formulations that are unconstrained by the form of the Helmholtz equations, and the authors propose a formulation that is more consistent than those most often used in that it includes implicit treatment of all terms associated with the pressure gradients and divergence. This formulation is stable for nonhydrostatic-scale simulations involving steep terrain, whereas the more common semi-implicit formulation is not. The ADI preconditioners are presented for use in simulations of both hydrostatic and nonhydrostatic scale flows. These simulations demonstrate the efficiency and accuracy of the preconditioned CR method and the overall stability of the model formulation. The simulations also suggest a general convergence criteria for the iterative algorithm in terms of the solution divergence.

1. Introduction

In the formulation of numerical models for time-dependent nonhydrostatic compressible atmospheric flow, acoustic waves impose a severe time-step restriction for algorithms using explicit time-integration methods. Buoyancy oscillations also restrict time steps for these algorithms in large-scale atmospheric flow applications. Techniques used to circumvent these time-step restrictions integrate terms responsible for the acoustic modes and buoyancy oscillations separately from, or in a different manner than, terms responsible for the resolved slower modes. In general, these methods can be categorized as either *split-explicit,* where acoustic and buoyancy terms are integrated explicitly with a smaller time step than the slow-mode terms, or *semi-implicit,* where the acoustic and buoyancy terms are integrated implicitly.

Split-explicit schemes are popular because they are generally efficient, easy to formulate and code, work well on nested grids, are well suited for adaptive models (which include overlapping grids, e.g., Skamarock and Klemp 1993), are easily mapped to MPP computer architectures, and can be used for models simulating a broad range of scales, from cloud to synoptic-scale flows. The leapfrog-based scheme of Klemp and Wilhelmson (1978) is perhaps the most popular split-explicit approach, and Skamarock and Klemp (1992) found that it is one of the few stable, robust split-explicit schemes available. However, while the split-explicit leapfrog-based models work well, it is not clear how to generalize the split-explicit approach to potentially more accurate or more efficient slow-mode integration methods. Skamarock and Klemp found that forward-in-time schemes (e.g., Crowley-type schemes) for integrating the compressible equations have considerable stability problems when combined with explicit time splitting. Other time-integration schemes, such as Adams–Bashforth and Runge–Kutta methods, share the stability problems of the forward-in-time schemes when used in concert with split-explicit integration of the acoustic modes, at least in their most straightforward implementations. Finally, we do not know how to combine a semi-Lagrangian integration with an efficient split-explicit formulation.

Corresponding author address: Dr. William C. Skamarock, NCAR/MMM Division, P.O. Box 3000, Boulder, CO 80307-3000.
E-mail: skamaroc@ncar.ucar.edu

Semi-implicit schemes have been somewhat less popular because of the difficulty involved in solving the 3D Helmholtz equation that arises in their formulation, although efficient 3D models do exist (e.g., Cullen 1990; Tanguay et al. 1990). These model formulations typically involve partitioning terms into those to be integrated explicitly and implicitly by making use of a 1D (in z) time-independent reference state. By design, the resulting Helmholtz equations are linear, have constant coefficients, and possess no cross-derivate terms (the terrain terms are handled explicitly). As such, they can be solved by a variety of methods. One of the primary advantages of the semi-implicit approach is that it allows a variety of integration methods for the slow modes. For example, a semi-implicit formulation naturally arises out of a semi-Lagrangian model formulation, and within an Eulerian semi-implicit formulation, forward-in-time and upwind-based integration methods can be used. However, the need for a tractable Helmholtz equation, brought about by the insufficiency of the Helmholtz solvers in use, has produced very complex model formulations. Moreover, there have been stability problems associated with the choice of the reference state that are not entirely understood (Cullen 1990; Golding 1992; Cullen and James 1994; Semazzi et al. 1995), and there are known stability problems with the explicit treatment of the terrain terms for nonhydrostatic simulations involving steep terrain (Ikawa 1988).

A more consistent way to formulate a semi-implicit compressible nonhydrostatic model, an approach not artificially constrained by concerns about the form of the Helmholtz equation, is to include all terms associated with the acoustic and buoyancy modes into the implicit scheme, and to temporally linearize only about a particular time step. In this way, no artificial reference state is needed, model formulations are simple, and the resulting models are stable and robust. In this paper we describe preconditioned conjugate-residual (CR) solvers that efficiently solve Helmholtz equations derived in this manner and demonstrate that these preconditioned CR solvers are efficient for cloud-scale, mesoscale, and large-scale simulation models.

We begin by presenting semi-implicit formulations for the fully compressible models in the next section that make use of the power and flexibility of the CR solvers. However, for the purpose of examining and understanding the behavior of the CR solvers, we also consider models based on the simpler nonhydrostatic compressible Boussinesq equations. Thus, we present in detail the continuous and finite-difference equations for a compressible Boussinesq model and derive the Helmholtz equation that arises in the semi-implicit discretization. We discuss the implicit differencing of the buoyancy in the vertical momentum equation and the vertical advection term in the thermodynamic equation that removes the Brunt–Väisälä frequency time-step restriction (typically $N\Delta t < 1$). In section 3 we outline the CR method analyzed in detail by Smolarkiewicz and Margolin (1994) and describe ADI preconditioners. Results from numerical tests confirming the efficiency and accuracy of the models are presented in section 4, where we demonstrate model efficiency in cloud-, meso-, and synoptic-scale simulations. A 2D model for the fully compressible (non-Boussinesq) equations is demonstrated. Convergence criteria for iterative solvers are discussed at the end of section 4 followed by a summary in section 5.

2. Equations

a. Fully compressible system

To illustrate the approaches taken in semi-implicit, nonhydrostatic compressible model formulation, it is sufficient to consider the fully compressible nonhydrostatic equations for 2D adiabatic flow. These equations, with the terrain-following coordinate transformation of Gal-Chen and Somerville (1975) as expressed in Durran and Klemp (1983), can be written as

$$\frac{\partial u}{\partial t} + c_p \theta \left(\frac{\partial \pi}{\partial x} + G \frac{\partial \pi}{\partial \zeta} \right) = -u \frac{\partial u}{\partial x} - \omega \frac{\partial u}{\partial \zeta} + D_u, \tag{1}$$

$$\frac{\partial w}{\partial t} + c_p \theta H \frac{\partial \pi}{\partial \zeta} - B = -u \frac{\partial w}{\partial x} - \omega \frac{\partial w}{\partial \zeta} + D_w, \tag{2}$$

$$\frac{\partial \theta}{\partial t} + w H \frac{\partial \theta}{\partial \zeta} = -u \frac{\partial \theta}{\partial x} - u G \frac{\partial \theta}{\partial \zeta} + D_\theta, \tag{3}$$

$$\frac{\partial \pi}{\partial t} + \frac{c_s^2}{c_p \theta} \left(\frac{\partial u}{\partial x} + G \frac{\partial u}{\partial \zeta} + H \frac{\partial w}{\partial \zeta} \right) + w H \frac{\partial \Pi_o}{\partial \zeta} = -u \frac{\partial \pi}{\partial x} - \omega \frac{\partial \pi}{\partial \zeta}, \tag{4}$$

where (u, w) are the Cartesian velocity components, the transformed coordinate

$$\zeta = \frac{z_t(z - z_s)}{z_t - z_s},$$

the coordinate transform terms $G = \partial\zeta/\partial x$ and $H = \partial\zeta/\partial z$, the "vertical" velocity in the transformed coordinate system $\omega = Gu + Hw$, $B = g(\theta/\theta_o - 1)$ is the buoyancy,

$$\Pi = \Pi_o(z) + \pi = \left(\frac{p}{p_o}\right)^{R/c_p},$$

the reference-state potential temperature

$$\theta_o(z) = -g\left(c_p\frac{\partial\Pi_o}{\partial z}\right)^{-1},$$

and D denotes the dissipation terms. Here, the introduction of the reference state is performed only to remove the large, canceling, hydrostatic terms in the vertical momentum equation.

Existing semi-implicit nonhydrostatic models (e.g., Cullen 1990; Tanguay et al. 1990) use the time-independent reference state to recast (1)–(4) as

$$\frac{\partial u}{\partial t} + c_p\theta_o\frac{\partial\pi}{\partial x} = -c_p\theta'\frac{\partial\pi}{\partial x} - c_p\theta G\frac{\partial\pi}{\partial\zeta} - \text{ADV}_u + D_u, \tag{5}$$

$$\frac{\partial w}{\partial t} + c_p\theta_o H\frac{\partial\pi}{\partial\zeta} - B = -c_p\theta'H\frac{\partial\pi}{\partial\zeta} - \text{ADV}_w + D_w, \tag{6}$$

$$\frac{\partial\theta}{\partial t} + wH\frac{\partial\theta_o}{\partial\zeta} = -u\frac{\partial\theta}{\partial x} - uG\frac{\partial\theta_o}{\partial\zeta} - \omega\frac{\partial\theta'}{\partial\zeta} + D_\theta, \tag{7}$$

$$\frac{\partial\pi}{\partial t} + \frac{c_o^2}{c_p\theta_o}\left(\frac{\partial u}{\partial x} + H\frac{\partial w}{\partial\zeta}\right) + Hw\frac{\partial\Pi_o}{\partial\zeta} = -\left(\frac{c^2}{c_p\theta} - \frac{c_o^2}{c_p\theta_o}\right)\left(\frac{\partial u}{\partial x} + H\frac{\partial w}{\partial\zeta}\right)$$
$$- \frac{c^2}{c_p\theta}G\frac{\partial u}{\partial\zeta} - \text{ADV}_\pi. \tag{8}$$

The left-hand-side (lhs) terms in (5)–(8) are integrated using an implicit formulation while the right-hand-side (rhs) terms are evaluated explicitly. The acoustic modes are associated with the pressure gradient terms in (5) and (6) together with the divergence term in (8). These terms on the lhs are linear, with a simple coefficient structure, while the terms on the rhs are generally nonlinear. Also, terms arising from the terrain transformation that would create cross derivative terms in the Helmholtz equation are handled explicitly. The buoyancy term in the vertical momentum equation (6) is handled implicitly along with the linearized vertical advection term in the θ equation (7). This part of the formulation removes the time-step restriction arising from gravity wave oscillations.

There are several potential difficulties with this approach. Stability with this partitioning of terms is not guaranteed. Partitioning problems with the terrain terms are discussed by Ikawa (1988), where he shows that this formulation is unstable for nonhydrostatic simulations using steep topography. The choice of θ_o can also affect the stability of the implicit buoyancy calculations (e.g., Cullen 1990; Golding 1992; Semazzi et al. 1995). Accuracy is also a concern when the reference state does not reasonably reflect the mean state of an evolving atmosphere.

A semi-implicit formulation more consistent and straightforward than (5)–(8) is to integrate (1)–(4) directly, with all terms on the lhs treated implicitly. The full pressure gradient and divergence terms along with the gravity wave terms are differenced implicitly with the understanding that the coefficients in front of the derivative terms in (1), (2), and (4) are evaluated explicitly. The coefficient structure of the Helmholtz equation is not regular and changes each time step, and all terrain terms are included in the implicit formulation. We have constructed a 2D model using this formulation and present results in section 4d.

b. Boussinesq model

Model formulation, efficiency, and accuracy are more easily addressed in the simpler Boussinesq framework, in which the fully compressible equations (1)–(4) are replaced by

$$\frac{\partial u}{\partial t} + H\frac{\partial\phi}{\partial x} + G\frac{\partial\phi}{\partial\zeta} = -u\frac{\partial u}{\partial x} - \omega\frac{\partial u}{\partial\zeta} + D_u, \tag{9}$$

$$\frac{\partial w}{\partial t} + H\frac{\partial\phi}{\partial\zeta} = -u\frac{\partial w}{\partial x} - \omega\frac{\partial w}{\partial\zeta}$$
$$+ D_w + B, \tag{10}$$

$$\frac{\partial B}{\partial t} = -u\frac{\partial B}{\partial x} - \omega\frac{\partial B}{\partial \zeta}$$
$$+ D_B, \tag{11}$$

$$\frac{\partial \phi}{\partial t} + c_s^2\left(\frac{\partial u}{\partial x} + G\frac{\partial u}{\partial \zeta} + H\frac{\partial w}{\partial \zeta}\right) = -u\frac{\partial \phi}{\partial x} - \omega\frac{\partial \phi}{\partial \zeta}. \tag{12}$$

In these equations $\phi = c_p\theta_o\pi$, $B = g(\theta - \theta_o)/\theta_o$, and the sound speed $c_s = 300$ m s^{-1}. We begin by first considering explicit integration of the buoyancy terms.

Semi-implicit discretization of the terms giving rise to the acoustic modes involves time averaging the terms on the left-hand sides of (9), (10), and (12). This discretization looks similar for both the three-time-level leapfrog schemes and the two-time-level forward-in-time schemes, and can be expressed compactly for the two-time level schemes on the C grid as

$$\delta u^n + \Delta t\beta\mathrm{PF}_x(\delta\phi^n) = \Delta t[-\mathrm{PF}_x(\phi^n)$$
$$- \mathrm{ADV}_u + D_u]$$
$$\equiv F_u, \tag{13}$$
$$\delta w^n + \Delta t\beta\mathrm{PF}_z(\delta\phi^n) = \Delta t[-\mathrm{PF}_z(\phi^n) - \mathrm{ADV}_w$$
$$+ D_w + \overline{B + \beta\delta B^n}^\zeta]$$
$$\equiv F_w, \tag{14}$$
$$\delta B^n = \Delta t(-\mathrm{ADV}_B + D_B), \tag{15}$$
$$\delta\phi^n + \Delta t\beta c_s^2\nabla\cdot(\delta\mathbf{v}^n) = \Delta t(-c_s^2\nabla\cdot\mathbf{v}^n - \mathrm{ADV}_\phi)$$
$$\equiv F_\phi. \tag{16}$$

In this formulation we are advancing the solution from time $n\Delta t$ to $(n + 1)\Delta t$ and all terms on the rhs are evaluated explicitly. The unknown variables are cast in terms of their differences as in Golding (1992); $\delta u^n = u^{n+1} - u^n$, $\delta w^n = w^{n+1} - w^n$, $\delta\phi^n = \phi^{n+1} - \phi^n$, and $\delta B^n = B^{n+1} - B^n$. The time-averaging parameter $\beta = 1/2$ represents centered averaging and $\beta = 1$ represents a fully implicit (backward) scheme. The pressure gradient terms

$$\mathrm{PF}_x(\phi) = \delta_x\phi + \overline{G\delta_{2\zeta}\phi}^x,$$
$$\mathrm{PF}_z(\phi) = H\delta_\zeta\phi,$$

the divergence operator

$$\nabla\cdot\mathbf{v} = \delta_x u + \overline{G\delta_{2\zeta}u}^x + H\delta_\zeta w,$$

$\delta_x = [\phi(x + \Delta x/2) - \phi(x - \Delta x/2)]\,\Delta x^{-1}$, likewise for δ_ζ, and $\mathbf{v} = (u, w)$. A leapfrog formulation of (14)–(16) requires a time step of $2\Delta t$, a redefinition of the general operator $\delta\psi^n = \psi^{n+1} - \psi^{n-1}$, the use of time level $n - 1$ in the rhs pressure gradient and divergence operators, replacement of the buoyancy term on the rhs of (14) with B^n, and changes to the advection and dissipation operators. Other semi-implicit formulations with different weightings of the $t + \Delta t$, t, and $t - \Delta t$ terms

(e.g., Coté et al. 1995) also produce formulations very similar to (13)–(16), including semi-Lagrangian formulations.

Time integration of (13)–(16) begins by advancing the explicit equation (15) followed by solving a Helmholtz equation for $\delta\phi^n$. We formulate an equation for $\delta\phi$, as opposed to the full pressure ϕ, to minimize cancelation errors and reduce the magnitude of the rhs terms in (13), (14), (16), and the Helmholtz equation. In the nonhydrostatic models of Cullen (1990), Tanguay et al. (1990) and others, the pressure equation is formed in terms of a difference from the linearly extrapolated value of $\phi^{n+1} = \phi^{n+1} - 2\phi^n + \phi^{n-1}$. We do not find that there is any significant advantage in using this form over $\delta\phi$ because the amount of additional cancelation in the rhs terms is small, both differences vanish for the steady-state problem, and most remaining benefits of using the extrapolated pressure can be gained by using $\delta\phi^n = \delta\phi^{n-1}$ as a first guess in the iterative CR solvers. Also, in a forward-in-time scheme, ϕ^{n-1} is not available unless explicitly saved.

The Helmholtz equation, derived by substituting for δu^n and δw^n from (14) and (15) into (16), is

$$c_s^2\beta^2\Delta t^2\nabla\cdot[\mathrm{PF}(\delta\phi^n)] - \delta\phi^n - R = 0, \tag{17}$$

where

$$R \equiv \Delta t\beta[\nabla\cdot(\mathbf{F}_v)] + F_\phi,$$

and $\mathbf{F}_v \equiv (F_u, F_w)$. Equation (17) can also be written in the form

$$L(\delta\phi^n) - R = 0, \tag{18}$$

where

$$L(\psi) \equiv c_s^2\beta^2\Delta t^2\,\nabla\cdot[\mathrm{PF}(\psi)] - \psi. \tag{19}$$

Equation (17) assumes an explicit discretization of the terms responsible for gravity oscillations, and the stability restriction for the entire scheme will be $N\Delta t < 1$ (see Skamarock and Klemp 1992). This approach is typically suitable for atmospheric models having grid lengths of a few tens of kilometers or less. For larger-scale models, the buoyancy term B in (10) and the vertical advection of the buoyancy, $wH(\partial B/\partial\zeta)$ in (11) can be differenced implicitly in order to circumvent this restriction, an approach first implemented by Cullen (1990) and Tanguay et al. (1990). In this approach (11) is recast as

$$\frac{\partial B}{\partial t} + Hw\frac{\partial B}{\partial \zeta} = -u\frac{\partial B}{\partial x} - Gu\frac{\partial B}{\partial \zeta} + D_B, \tag{20}$$

and (15) is replaced with the finite-difference representation of (20)

$$\delta B^n + \beta\Delta t\overline{\delta w^n H\delta_\zeta B^n}^\zeta = \Delta t(-\mathrm{HADV}_B + D_B)$$
$$\equiv F_B, \tag{21}$$

where the advection term HADV includes the advection

terms on the rhs of (20). The discretized vertical momentum equation becomes

$$\delta w^n + \Delta t \beta[- \text{PF}_z(\delta\phi^n) - \overline{\delta B^n}^\zeta]$$
$$= \Delta t[\text{PF}_z(\phi^n) - \text{ADV}_w + \text{D}_w + \overline{B^n}^\zeta]. \quad (22)$$

The solution procedure for the new system, (13), (16), (21), and (22), is to eliminate δB^n from (22) using (21), and then solve the Helmholtz equation formed by substituting the revised equation (22) and (13) into (16). A problem arises, however, when combining (21) and (22). The new discretized momentum equation, with δB^n eliminated, becomes

$$\delta w^n + \Delta t^2 \beta^2 \overline{\delta w^n H \delta_\zeta B^n}^{\zeta\zeta} + \Delta t \beta \text{PF}_z(\delta\phi^n)$$
$$= \Delta t[-\text{PF}_z(\phi^n) - \text{ADV}_w + \text{D}_w + \overline{B^n + \beta F_B}^\zeta]$$
$$\equiv F_w^*. \quad (23)$$

The unknown δw^n in (23) is averaged twice in ζ, and the matrix representation of the vertical discretization of (23) would have to be inverted in order to eliminate δw^n from the pressure equation (16) using (23). The resulting Helmholtz equation would be very complex. Cullen (1990) and Tanguay et al. (1990) circumvent this problem by lumping all the δw^n terms on to the diagonal, such that

$$\delta w^n + A^{-1}\Delta t\beta \text{PF}_z(\delta\phi^n) = A^{-1}F_w^*, \quad (24)$$

where

$$A \equiv 1 + \beta^2\Delta t^2\overline{H\delta_\zeta B^n}^{\,\zeta\zeta}.$$

The Helmholtz equation derived by substituting (13) and (24) into (16) has the same form as (17) except that the vertical pressure gradient $\text{PF}_z(\phi) = A^{-1}H\delta_\zeta\phi$ and $A^{-1}F_w^*$ replaces F_w. This difficulty arising from the $\overline{\delta w}^{\zeta\zeta}$ term is a result of the Lorenz grid vertical staggering. No problem arises if θ and w are collocated as in the Charney–Phillips vertical staggering (Cullen and James 1994; Semazzi et al. 1995).

3. Conjugate-residual solver and preconditioners

a. Conjugate-residual solver

The basic CR solver we use is a special case of the truncated generalized conjugate residual, GCR(k), method of Eisenstat et al. (1983), which is a nonsymmetric variant of the conjugate gradient (CG) approach. As discussed in Smolarkiewicz and Margolin (1994), CG algorithms can be interpreted physically as finite-difference schemes for integrating (in a pseudo-time to a steady state) a damped oscillation equation with forcing equal to the residual error $r \equiv L(\psi) - R$ of the linear elliptic problem $L(\psi) = R$. Arbitrary coefficients multiplying pseudo–time derivatives of the oscillation equation, as well as the pseudo–time step of the integration, are derived variationally for each iteration by minimiz-

TABLE 1. The preconditioned conjugate-residual (CR) scheme.

initialize r_i^0, $p_i^0 = P_i^{-1}(r^0)$, $L_i(p^0)$	
begin loop ν	
$\beta = -\dfrac{\langle r^{\nu-1}L(p^{\nu-1})\rangle}{\langle L(p^{\nu-1})L(p^{\nu-1})\rangle}$	(26a)
$\psi_i^\nu = \psi_i^{\nu-1} + \beta p_i^{\nu-1}$	(26b)
$r_i^\nu = r_i^{\nu-1} + \beta L_i(p^{\nu-1})$	(26c)
exit loop if $\|r^\nu\| \le \epsilon$	
$q_i^\nu = P_i^{-1}(r^\nu)$	(26d)
evaluate $L_i(q^\nu)$	(26e)
$\alpha = -\dfrac{\langle L(q^\nu)L(p^{\nu-1})\rangle}{\langle L(p^{\nu-1})L(p^{\nu-1})\rangle}$	(26f)
$p_i^\nu = q_i^\nu + \alpha p_i^{\nu-1}$	(26g)
$L_i(p^\nu) = L_i(q^\nu) + \alpha L_i(p^{\nu-1})$	(26h)
end loop	

ing a selected error norm. Given certain properties of L, this assures optimal convergence (in the selected norm) of the subsequent iterates to the solution of the elliptic problem at hand. Depending upon the particular form of the finite-difference approximation of the oscillation equation and the selected norm, a variety of CG schemes can be derived. We use CR schemes that minimize the mean square residual $\|r\|_2$. These schemes do not require (for their monotone convergence) the symmetry of the matrix representing L on the grid—a necessary assumption for the validity of the classical CG scheme of Hestenes and Stiefel (1952). This makes CR schemes especially well suited for solving complex elliptic problems typical in modeling atmospheric flows (Kapitza and Eppel 1992; Smolarkiewicz and Margolin 1994).

The GCR(k) algorithm employs the kth-order oscillation equation, and the basic CR scheme employed in this paper utilizes the second-order equation

$$\frac{\partial^2\psi}{\partial\tau^2} + \frac{1}{T}\frac{\partial\psi}{\partial\tau} = L(\psi) - R, \quad (25)$$

where $T(\tau)$ is an arbitrary coefficient. Standard finite-difference discretization of the pseudo–time derivatives on the lhs of (25), forming the associated scheme for r [in essence, by acting with L on both sides of the finite-difference form of (25)], and the variational determination of the two coefficients (related to T and $\Delta\tau$) by minimizing $\|r\|_2$ lead (cf. sections 2 and 3 in Smolarkiewicz and Margolin 1994) to the elementary CR algorithm (Stiefel 1955) summarized in Table 1 (where the preconditioner $P \equiv P^{-1} \equiv I$, the identity matrix; preconditioners will be discussed in the next section).

In Table 1, subscript $\mathbf{i} \equiv [i, j, k]$ denotes the discrete representation of a field on the grid, and $\langle\xi\zeta\rangle \equiv \Sigma_i\xi_i\zeta_i$ symbolizes the inner product. To integrate the discretized counterpart of (25) to steady state without preconditioning ($P \equiv I$), one begins with an initial guess ψ_i^0, and initializes accordingly the residual error $r_i^0 =$

$L_i(\psi^0) - R_i$ and the auxiliary variable p_i (often referred to as the direction vector) $p_i^0 = r_i^0$. The residual error measures how well a solution satisfies the elliptic problem at hand, whereas the direction vector measures the rate of change of the residual error itself. For negative definite L (i.e., for dissipative, "energy" decreasing operators) the problem is well behaved, and successive trial solutions ψ_i^ν in (26b) [see Table 1 for Eqs. (26a)–(26h)] produce successively smaller solution errors in (26c), as measured by $\| r \|_2$. As each solution is generated, an arbitrary error norm can be evaluated and, when this error norm is sufficiently small, the latest trial solution is taken as the converged result.

Several features of the CR algorithm make it attractive for use in solving the discrete Helmholtz equation (17). First, the operator L is never explicitly inverted and its exact form need not be explicitly coded. In our models we use the subroutines that compute the pressure gradients and divergence in the momentum and pressure equations to evaluate $L(\psi)$. After two evaluations of the operator L in the computation of r^0 and $L(p^0)$ in the initialization, there remains only one evaluation of the operator (26e) for each CR iteration; the other evaluation of L is computed using the recursion relation (26h) and the new residual is computed using the recursion relation (26c).

b. Preconditioners

The common perception of CG methods is that to be truly effective they require acceleration by some preconditioner, and we have found this to be true for our problem. A preconditioner recasts the oscillation equation (25) into

$$\frac{\partial^2 P(\psi)}{\partial \tau^2} + \frac{1}{T}\frac{\partial P(\psi)}{\partial \tau} = L(\psi) - R,$$

where P is the preconditioning operator (i.e., preconditioner). The resulting preconditioned basic CR scheme has been summarized in Table 1. There is no general method for designing an optimal preconditioner (Axelsson 1994, section 7). In the CR scheme (26), the preconditioner P can be, in principle, any linear operator such that LP^{-1} is definite. Its goal, however, is to augment the governing problem $L(\psi) - R = 0$ with an auxiliary problem $P^{-1}[L(\psi) - R] = 0$, which converges faster than the original problem due to a closer clustering of the eigenvalues of the auxiliary elliptic operator $P^{-1}L$. For the preconditioner to be useful, the convergence of the auxiliary problem must be sufficiently rapid to overcome the effort associated with inverting P in (26d). In general, the closer P approximates L, the faster CR converges but the more difficult it will be to invert P. For example, in the $P \equiv L$ limit, CR converges in one iteration but the entire effort of solving the elliptic problem is placed into inverting P (bringing us back to the starting point), whereas in the $P \equiv I$ limit, inverting P is trivial but there is no acceleration of the CR scheme.

In between, there is great flexibility in designing preconditioners exploiting either direct or relaxation methods in step (26d) of the CR procedure. This flexibility adds a degree of freedom to the design of conjugate gradient methods, which itself constitutes an established area of research (see Axelsson 1994 for a review).

The preconditioner we use is the ADI method, which seeks the solution to (26d) by advancing the pseudo-time-dependent problem

$$\frac{\partial q}{\partial \eta} = P(q) - r \tag{27}$$

to steady state, performing an implicit pseudo-time η integration alternately in each coordinate direction. A succinct review of ADI methods for solving elliptic equations is given in Roache (1972), and we follow the classical ADI discretization.

For simplicity, consider as an analog to (27) the simple heat equation

$$q_\eta - D(q_{xx} + q_{zz}) = r.$$

Here, the subscripts denote partial differentiation and D is a constant heat conductivity. The finite-difference ADI formulation can be expressed as

$$(I - \beta_1\delta_{xx})q^{\mu+1/2} = (I + \beta_2\delta_{zz})q^\mu + \frac{\Delta\eta}{2}r \tag{28a}$$

$$(I - \beta_2\delta_{zz})q^{\mu+1} = (I + \beta_1\delta_{xx})q^{\mu+1/2} + \frac{\Delta\eta}{2}r, \tag{28b}$$

where $\beta_1 \equiv D\Delta\eta/2\Delta x^2$, $\beta_2 \equiv D\Delta\eta/2\Delta z^2$, $\delta_{xx}q \equiv q_{i-1,k} - 2q_{i,k} + q_{i+1,k}$, and $\delta_{zz}q \equiv q_{i,k-1} - 2q_{i,k} + q_{i,k+1}$.[1] The free parameter in this problem is $\Delta\eta$, and one wishes to choose it such that the steady state is approached in the fewest number of steps. The most efficient implementations of ADI will cycle around a number of values of $\Delta\eta$.

Used as an elliptic solver, ADI advances a pseudo-time-dependent equation to steady state. However, it need not be iterated to the convergence when used as a preconditioner in (26d). One ADI iteration per CR iteration is sufficient to substantially accelerate the CR scheme. Thus, we do not completely invert the operator P in (27) but only use the approximate inversion produced by the single sweep of the ADI scheme [(28a) and (28b)]. Also, as we shall demonstrate in the next section, abbreviated operators $P \approx L$ in (27) accelerate convergence as well, while simplifying the design and overall efficiency of the ADI preconditioner. Hence the ADI preconditioner contains two levels of approximation; P only approximates L in (27), and the single ADI sweep only approximates P^{-1}.

---

[1] Three-dimensional ADI schemes are not straightforward extensions of the two-dimensional factorization presented here; the straightforward extension is unstable. Readers should refer to Roache (1972) or Douglas (1962) for a discussion of stable factorizations.

In cases where the flow is largely hydrostatic (typically in model configurations using large grid aspect ratios $\Delta x/\Delta z$), we have found that using the ADI preconditioner with only the vertically implicit element retained [using (28b) without (28a) and setting $q^{\mu+1/2} = q^{\mu}$] significantly increases the efficiency of the preconditioned ADI scheme. With large grid aspect ratios, the coefficients multiplying the vertical second derivatives will be much greater than those multiplying the horizontal derivatives (the coefficient is proportional to the square of the aspect ratio), and this modified ADI proves efficient. The one-dimensional ADI preconditioner also accelerates the CR scheme when grids are isotropic ($\Delta x \sim \Delta z$), but the full ADI accelerates the CR scheme substantially more on isotropic grids. In all cases we use an initial guess $q^0 = 0$ in the ADI, and we have not found a different initial guess that further accelerates the CR-ADI scheme.

The 1D ADI preconditioner is similar to the hydrostatic preconditioner in a conjugate gradient solver for the Poisson equation used by Hill and Marshall (1995) in an incompressible nonhydrostatic ocean model (hydrostatic in that the preconditioner gives the exact solution in the hydrostatic limit). The efficiency of their preconditioner suggests that a number of efficient preconditioners exist for any particular problem. The ADI is, perhaps, a more flexible preconditioner for the compressible system, particularily in the case where flows are significantly nonhydrostatic. Also, the CR solver does not require a symmetric Helmholtz problem, whereas the conjugate gradient method used by Marshall et al. requires a symmetric Poisson problem.

4. Numerical examples

a. Accuracy

The efficiency and accuracy of split-explicit formulations for a Boussinesq model were examined in Skamarock and Klemp (1994), where numerical simulations of small amplitude propagating inertia–gravity waves were compared with analytic solutions to the linearized equations for both nonhydrostatic and hydrostatic flow regimes. Herein, we compare solutions from the leapfrog semi-implicit Boussinesq model described in section 2b with those analytic solutions and the split-explicit model solutions in order to verify the accuracy and efficiency of the CR scheme. In constructing the semi-implicit models, all we have done is replace the small-time-step code in the split-explicit model with the semi-implicit code.

The analytic solutions are given in Skamarock and Klemp (1994) and are depicted in Fig 1. The waves are excited by an initial θ perturbation 10^{-2} K. For the nonhydrostatic waves, the periodic channel has a length of 300 km, a height of 10 km, $\Delta x = \Delta z = 1$ km, and a mean advection speed of $U = 20$ m s^{-1} is prescribed along with an initial perturbation half-width of 5 km.
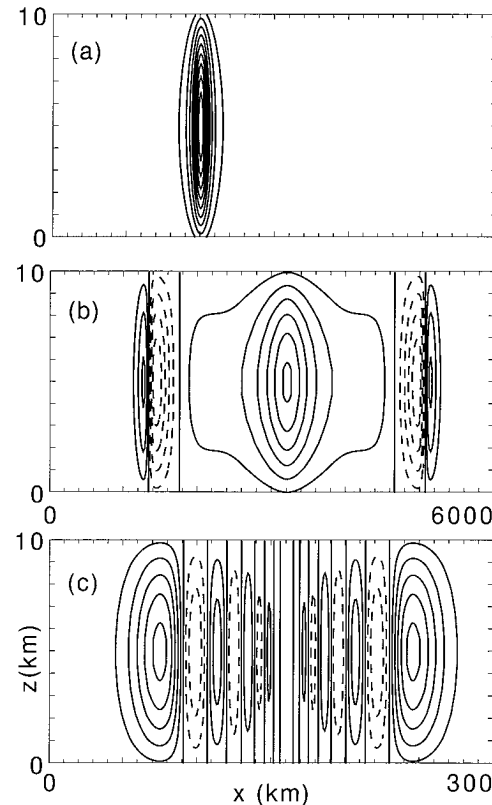

FIG. 1. Perturbation θ (a) at $t = 0$ for the hydrostatic- and nonhydrostatic-scale inertia–gravity wave simulations plotted with a contour interval of 10^{-3} K. The analytic solution for (b) the hydrostatic wave at 60 000 s, and (c) the nonhydrostatic wave at 3000 s, both plotted with a contour interval of 0.5×10^{-3} K. Negative contours are dashed.

For the hydrostatic waves, the periodic channel has a length of 6000 km, a height of 10 km, $\Delta x = 20$ km, and $\Delta z = 1$ km. Again, a mean advection speed of $U = 20$ m s^{-1} is used and the initial perturbation half-width is 100 km. Figures 2a and 2b depict the rms error in the θ fields from the model solutions for the nonhydrostatic and hydrostatic simulations, respectively. The semi-implicit model is generally as accurate as the split-explicit model in both cases.

The results in Figs. 2a and 2b are computed using conservative convergence criteria in the CR Helmholtz solver. Obviously, one does not want to expend more effort solving the Helmholtz equation than necessary, but without recourse to comparison with an exact solution we must look elsewhere for a measure of the solution accuracy. Figures 3a and 3b present the error at the end of the simulations with the semi-implicit model versus the CR convergence criteria. In this comparison we nondimensionalize the Helmholtz equation (17), dividing by c_s^2, and the convergence criteria used is that the maximum absolute value of the dimensionless residual be less than ϵ. In both cases the solution error is unchanged when ϵ is at or below a value ϵ_c. We define
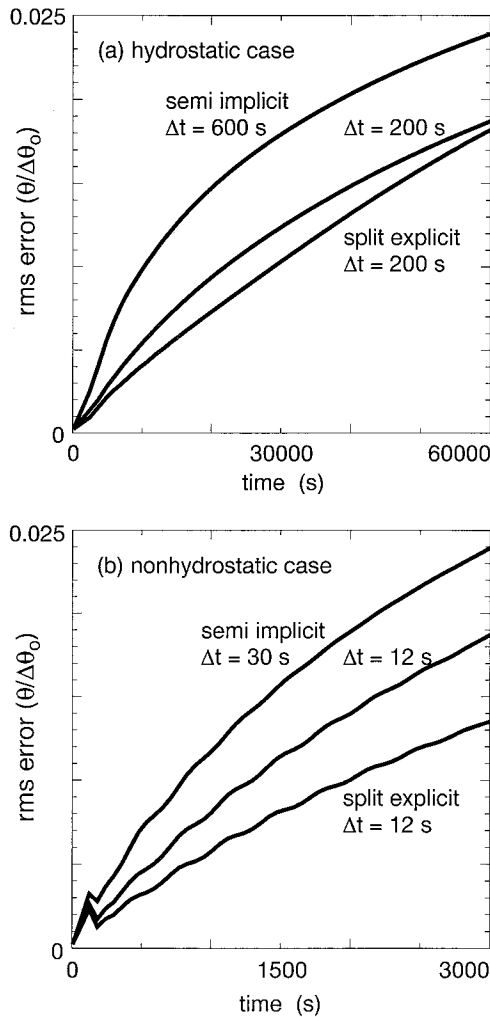
FIG. 2. Normalized rms errors for (a) the hydrostatic and (b) the nonhydrostatic inertia–gravity wave simulations.

ϵ_c to be the value of epsilon below which the solution error remains unchanged and the point at which CR iterations should cease. We discuss a priori estimates of ϵ_c in section 4e. We have also plotted the rms divergence as a function of the convergence parameter ϵ in Figs. 3a and 3b. The divergence is and should be nonzero in the compressible system, and we find that the rms divergence parallels the solution error. It is constant for values of ϵ less than ϵ_c, and grows for $\epsilon > \epsilon_c$. In simulations where we do not have the exact solution, we find that the divergence exhibits behavior similar to this case. Hence, we will take ϵ_c to be the value of ϵ at which the solution divergence begins to increase.

We show the CPU time and iteration count for the nonhydrostatic and hydrostatic simulations in Table 2,[2]

---

[2] The simulations were performed on an SGI R4400 workstation. The split-explicit model results reflect a 50% speed increase over the SGI R4000 workstation used in Skamarock and Klemp (1994).
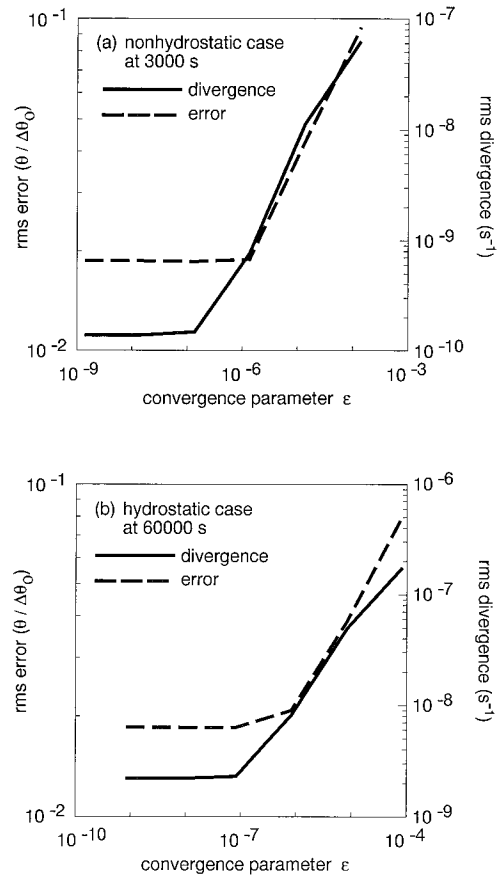

FIG. 3. The rms errors and rms divergence for (a) the hydrostatic and (b) the nonhydrostatic inertia–gravity wave simulations.

and compare these with the split explicit model results. The unpreconditioned conjugate residual scheme is reasonably efficient for these problems because the cost of a CR iteration is approximately that of a small (acoustic) time step in the split-explicit model. Given that the number of small time steps per $2\Delta t$ leapfrog time step in the split-explicit models is of order 10, the CR convergence in order 10 iterations should be efficient. Also, we have simulated the hydrostatic inertia–gravity wave with a 600-s time step and plotted the results in Fig. 2a. For the explicit buoyancy scheme (14) and (15), the maximum time step is 200 s ($N\Delta t < 2$ for the leapfrog model), but for the implicit buoyancy scheme there is no time step restriction based on the buoyancy oscillations, although the solution error increases because of the larger time step. We have also run the nonhydrostatic CR simulation with a larger time step (Fig. 2b), and the result has shown larger solution error. The cost of the simulations, including the total number of CR iterations needed, is less in the simulations using the larger time step as evidenced in both the hydrostatic and nonhydrostatic cases (see Table 2). This is not generally the case; more often we find that a larger time step increases

TABLE 2. Inertia–gravity wave simulation statistics for the unpreconditioned CR solver.

	ϵ	Δt (s)	Time steps	CR iterations per acoustic steps per time step	Non-acoustic CPU (s)	Acoustic CPU (s)	Total CPU (s)
Hydrostatic inertia–gravity wave							
Split-explicit		200	300	10	4.37	15.42	19.79
Semi-implicit	1.4×10^{-7}	200	300	10.7	4.32	16.88	21.20
θ-explicit	1.4×10^{-8}	200	300	18.3	4.32	26.79	31.11
Semi-implicit	1.4×10^{-7}	200	300	9.4	4.05	18.06	20.11
θ-implicit	1.4×10^{-8}	200	300	11.0	4.13	20.26	24.39
	4.2×10^{-8}	600	100	16.8	1.46	9.41	10.87
	4.2×10^{-9}	600	100	25.4	1.33	13.26	14.60
Nonhydrostatic inertia–gravity wave							
Split-explicit		12	250	8	3.71	10.18	13.89
Semi-implicit	8.0×10^{-8}	12	250	9.5	3.53	12.88	16.41
θ-implicit	8.0×10^{-9}	12	250	15.5	3.62	9.77	23.39
	2.0×10^{-8}	30	100	10.3	1.46	12.19	13.65

the total number of CR iterations needed for a simulation.

b. Preconditioners for the terrain formulation and time-step considerations

The previous examples involved a very simple Helmholtz equation; the simulations included no orography and the coefficients in the Helmholtz equation were constant. The semi-implicit model did not require preconditioning in the CR scheme for efficiency. Here, we simulate essentially hydrostatic and strongly nonhydrostatic nonlinear mountain waves and we find CR preconditioning is necessary for model efficiency; 1D (only vertically implicit) ADI is found to be the most efficient preconditioner for anisotropic grids (the hydrostatic mountain-wave case) and multidimensional

FIG. 4. Hydrostatic-scale mountain wave simulation at 40 000 s. The potential temperature θ is contoured in gray with an interval of 0.5 K. The vertical velocity is contoured with an interval of 0.2 m s^{-1}. The plotted region is 800 km × 10 km.

ADI is found to be most efficient for isotropic grids (the nonhydrostatic case). In this section, we also consider model formulations where cross-derivative terms are included in the Helmholtz equation.

Figure 4 shows a mountain wave solution at 40 000 s, just prior to wave breaking, for flow over a bell-shaped mountain of half-width 50 km and height 1 km embedded in a mean flow of 20 m s^{-1} with a constant atmospheric stability of $N = 0.02$ s^{-1}. The model configuration is $\Delta x = 10$ km and $\Delta z = 420$ m (101 × 45 grid points), and $\Delta t = 50$ s. In these simulations we are using a forward-in-time two-time-level model with the elementary second-order Crowley scheme for advection. The flow is very nearly hydrostatic with the 50-km half-width, and we precondition using ADI with only a single implicit z sweep with $\beta_2 = 75$ in (28b) (see section 3b). We have verified that we do not need to include the cross-derivative terms in the preconditioner (cf. Bernadet 1995); preconditioners that include the cross-derivative terms do not perform better and are more than twice as expensive per preconditioning sweep. Figure 5a shows the rms divergence as a function of the convergence parameter ϵ and also presents the CR iterations for the convergence parameter using both the unpreconditioned and the preconditioned CR. An ADI preconditioning sweep, using (28b), cost significantly less than a small time step in the split-explicit model or a CR iteration in the semi-implicit model, thus we find that the model is efficient with preconditioning given that fewer than ten preconditioned CR iterations are needed per time step. The unpreconditioned model is not efficient; at the minimum convergence level ($\epsilon \sim 10^{-6}$ in Fig. 5a), approximately 50 unpreconditioned CR iterations are needed per time step versus 5 for the preconditioned scheme.

To further examine the preconditioner, we have reduced the mountain width to 5 km, and set $\Delta x = 1$ km.

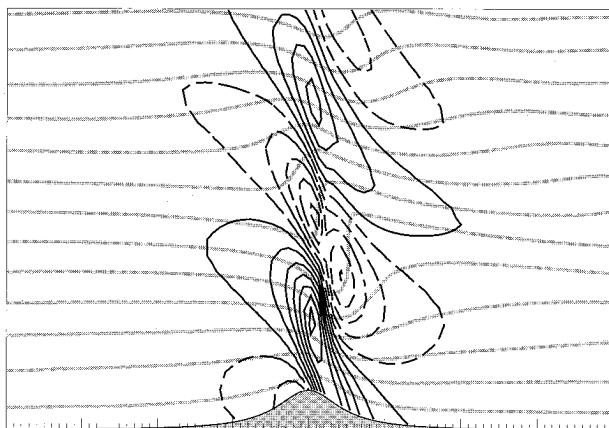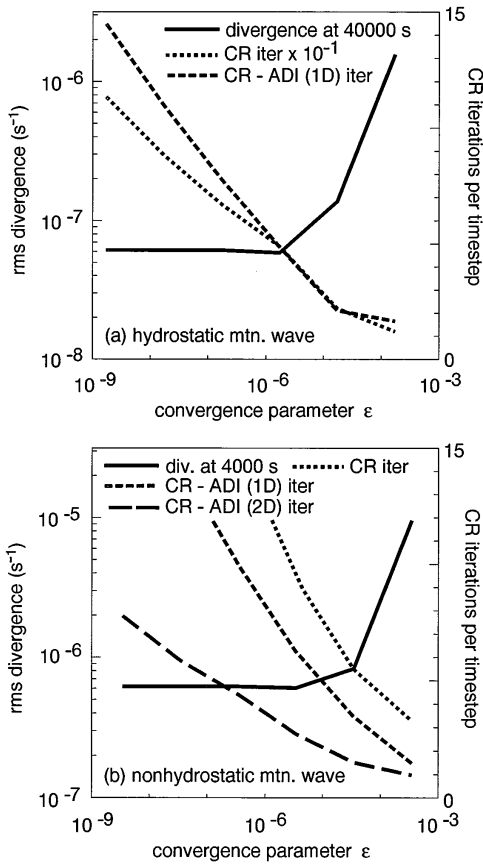FIG. 5. The rms divergence and average number of CR iterations per time step for (a) the hydrostatic and (b) the nonhydrostatic mountain wave simulations. The CR iterations for the unpreconditioned CR in the hydrostatic case are multiplied by 10^{-1}.

In this formulation, the largest value of the coefficient G in (9) is 0.25, which produces a significant cross-derivative term in the Helmholtz equation. Figure 5b shows the maximum divergence as a function of the convergence parameter ϵ, and also presents the CR iterations for the convergence parameter using both the unpreconditioned and the preconditioned CR. Figure 5b depicts results for both full and vertically implicit-only ADI preconditioning. Both preconditioners dramatically accelerate the CR scheme, with the full ADI preconditioner generally requiring half the number if CR iterations for convergence compared with the vertically implicit-only preconditioner. Again, we verify that the cross-derivative terms need not be included in the preconditioner, even here in the case where they have coefficients of $O(1)$. The model is efficient in this simulation [a preconditioning sweep using (28b) and/or (28a) without the cross-derivative terms is still less expensive than a split-explicit small time step or a CR iteration]. Moreover, the model is stable for this simulation, whereas semi-implicit formulations that handle the terrain terms explicitly would be unstable (Ikawa 1988).

We have also integrated a leapfrog semi-implicit for-

mulation of the terrain model, and have varied the time steps in both the leapfrog and forward-in-time models. The results show that the CR iterations scale roughly with the time step, that is, a doubling of the time step size leads to doubling the number of CR iterations required to reach a specified convergence level. This result is independent of preconditioner use. In the leapfrog formulation, the effective time step of the semi-implicit portion of the scheme is $2\Delta t$, while the effective time step for the forward-in-time scheme is Δt. Thus, assuming all other elements remain unchanged, the CR solution in the forward-in-time model will require half the cost of the corresponding leapfrog-model solution. Numerical simulations with a leapfrog semi-implicit terrain model for these cases confirm this. However, the generality of these results is not certain given the results from the inertia–gravity wave tests (section 4a, Table 2) in which the number of CR iterations did not scale directly with the time step.

c. Efficiency for large problems

The cost per time step of conjugate residual schemes is roughly proportional to $n\sqrt{\kappa}$ (e.g., $n\sqrt{n}$ in a simple 2D elliptic problem), where n is the number of points in the solution domain and κ is the condition number of the matrix representing the discretized elliptic problem (Stoer 1983). This cost can render high-resolution simulations prohibitively expensive, especially compared with the cost of a time step in the split-explicit models, proportional to n, and the cost of direct methods for solving Helmholtz equations, generally proportional to $n \log(n)$. Our experience is that the preconditioners reduce the costs of the simulations to where they are more nearly proportional to $n \log(n)$; the number of iterations is only weakly dependent on problem size.

To illustrate this behavior (as well as to examine the robustness of our approach for strongly nonlinear flows and to again verify the implicit buoyancy formulation) we have performed 3D simulations of baroclinic waves with the Boussinesq model. These simulations, carried out originally by Rotunno et al. (1995) using a split-explicit model formulation, are performed on low and high resolution grids ($41 \times 81 \times 61$ grid points, $\Delta x = \Delta y = 100$ km, $\Delta z = 250$ m, $\Delta t = 450$ s, and $161 \times 321 \times 61$ grid points $\Delta x = \Delta y = 25$ km, $\Delta z = 250$ m, $\Delta t = 90$ s, respectively) with and without preconditioning of the CR solver. Figure 6a depicts the rms divergence as a function of ϵ for a selected time in two of these simulations. Again, the divergence is constant for $\epsilon < \epsilon_c$ and increases for $\epsilon > \epsilon_c$. Also shown is the number of CR iterations necessary to achieve a convergence level ϵ without and with the preconditioner (Fig. 6b), in this case the ADI using only the a single z-implicit pass per CR iteration (28b) and the coefficient $\beta_2 = 100$. The nonpreconditioned CR takes an inordinate number of iterations, while the preconditioned CR takes only a small number of iterations to reach con-
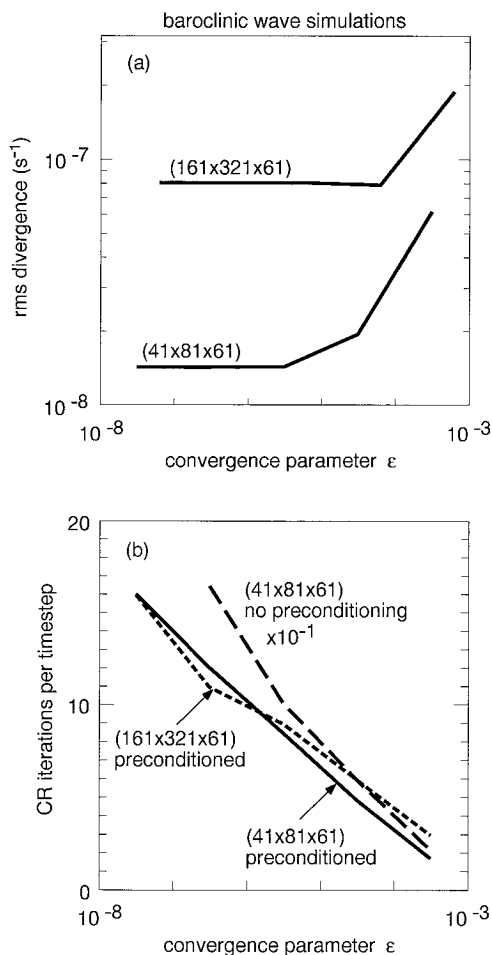
FIG. 6. (a) The rms divergence and (b) the average number of CR iterations per time step for the coarse- and fine-resolution baroclinic wave simulations. The CR iterations for the unpreconditioned CR are multiplied by 10^{-1}.
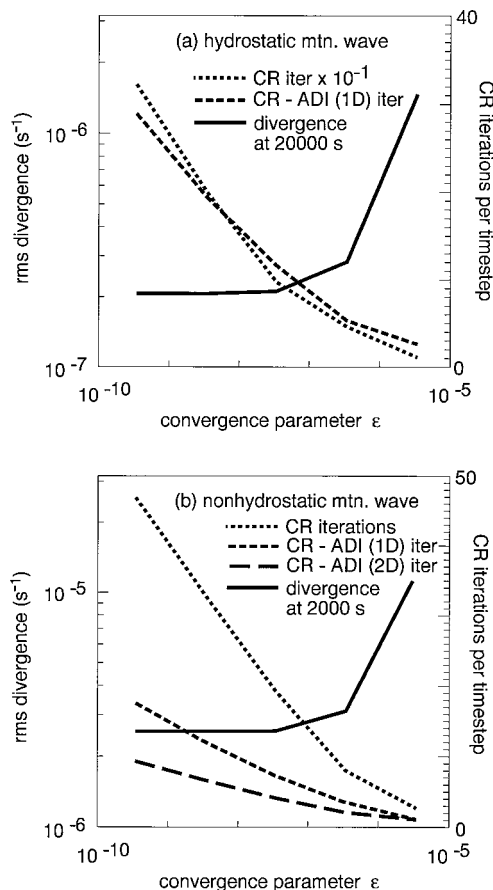

FIG. 7. The rms divergence and average number of CR iterations per time step for (a) the hydrostatic and (b) the nonhydrostatic mountain wave simulations using the fully compressible model. The CR iterations for the unpreconditioned CR in the hydrostatic wave simulations are multiplied by 10^{-1}.

vergence. Intuitively, we believe that the ADI preconditioner quickly finds the hydrostatic component of the solution; for the large Δx and large aspect ratios in these simulations ($\Delta x / \Delta z = 400, 100$) the solution is essentially hydrostatic. We have found that this preconditioner is efficient for all flows that are essentially hydrostatic (typically simulations with $\Delta x \geq 5$ km).

We have also performed simulations of buoyant thermals at nonhydrostatic scales in three spatial dimensions and find the same general behavior. The number of CR iterations is only weakly dependent on problem size, and the preconditioned CR method remains efficient even for large problems. As in the nonhydrostatic-scale mountain wave simulations, multidimensional (3D) ADI was used, in this case incorporating the factorization described in Roache (1972, 94).

d. Fully compressible terrain model

We have constructed a 2D terrain model using the full equations based on the formulation described in

section 2a where we solve (1), (2), (4), and (9). In the pressure gradient terms and divergence terms θ at time t is used, and π at time t is used to evaluate the sound speed c_s^2. We also use θ at time t in the implicit treatment of the vertical advection of θ (used to circumvent the gravity wave time-step restriction). For flows in which θ and π possess structure at all scales, the coefficients in the Helmholtz equation will contain structure at all scales, and we wish to determine whether this effects the efficiency of the CR solver and the relationship of the divergence to the convergence parameter ϵ.

We have repeated the mountain wave simulations presented in section 4b using this model. The results are similar except that the wave amplitude differs given the variation of density with height, and the wave overturns sooner. Figure 7 shows the maximum divergence as a function of the convergence parameter ϵ, and also presents the CR iterations as a function of the convergence parameter using both the unpreconditioned and the preconditioned CR for both the hydrostatic- and nonhy-

drostatic-scale simulations. The divergence for the fully compressible model,

$$\frac{\partial u}{\partial x} + G\frac{\partial u}{\partial \zeta} + H\frac{\partial w}{\partial \zeta} + \left(\frac{c_s^2}{c_p\theta}\right)^{-1} wH\frac{\partial \Pi_o}{\partial \zeta},$$

exhibits the same behavior as in the Boussinesq case; that is, its rms value is constant for ϵ less than some critical value and rises for $\epsilon > \epsilon_c$. The preconditioners are as effective as in the Boussinesq cases and the total number of iterations needed for acceptable convergence using the preconditioned CR scheme is $O(10)$. The full ADI preconditioner is significantly more efficient than the vertically implicit-only ADI preconditioner for the relatively isotropic grid (Fig. 7b), as was the case in the Boussinesq simulations (Fig. 5b).

e. Convergence criteria

The overall solution error can be affected by the error in the Helmholtz solution; however, at some point (at ϵ_c in our examples) increased accuracy of the Helmholtz solution does not result in increased accuracy of the model solution. We seek an a priori estimate of ϵ_c to facilitate general use of a compressible model that uses the CR solver. In the anelastic system, Smolarkiewicz et al. (1997) stops the CR iterations when the divergence is sufficiently small such that spurious divergence in the anelastic momentum and thermodynamic equations results in solution errors below the truncation errors of those discretizations. This and other heuristic arguments lead to the general result that $\Delta t \, \text{div}(\mathbf{V}) < \epsilon \min(C, L)$, where C and L are the magnitudes of the Courant and Lipschitz numbers, $C = \|\Delta t \mathbf{V}/\Delta x\|$ and $L = \|\Delta t(\partial \mathbf{V}/\partial \mathbf{x})\|$. Generally, $\epsilon < 10^{-3}$, 10^{-4} is sufficient in semi-Lagrangian models, although smaller values of ϵ may be necessary in Eulerian models.

The divergence is nonzero in the compressible system, and we cannot directly appeal to the divergence-based arguments in Smolarkiewicz et al. We find, however, that a convergence criteria similar to Smolarkiewicz et al. can be constructed for all the simulations we have performed. The convergence level ϵ_c takes the form

$$\epsilon_c \sim \delta\frac{u'\Delta t}{\Delta x}, \tag{29}$$

where u' is the perturbation velocity in the system, that is, it is not the mean wind in the system but rather it is the perturbation wind (typically $u_{max} - u_{min}$). An order of magnitude estimate of the perturbation velocities appears sufficient to generate reasonable estimates for the rms divergence. In the inertia–gravity wave simulations, for example, the perturbation velocity 10^{-2} m s^{-1} is three orders of magnitude smaller than the mean advection velocity $U = 20$ m s^{-1}. Here, δ is the scaling factor for the divergence in (29), and we use $\delta \approx 5 \times 10^{-3}$. The scaled divergence data from all our simulations, along with the scaling velocities, are given in Fig. 8. The
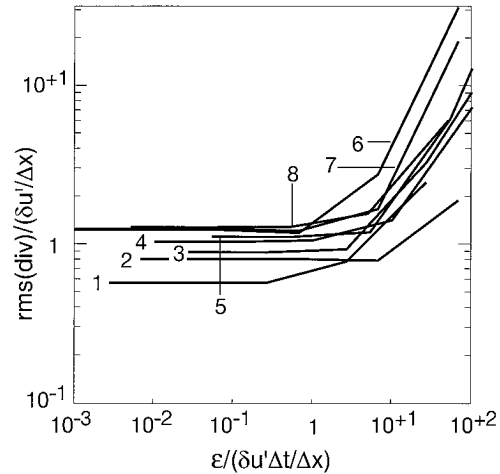

Fig. 8. Normalized rms divergence versus the normalized convergence parameter for all simulations. The scaling velocities u' are 10^{-2} m s^{-1} for the inertia–gravity wave simulations, 1 m s^{-1} for the mountain wave simulations, and 10 m s^{-1} for the baroclinic wave simulations. The data are 1) the baroclinic wave coarse-grid and 2) fine-grid simulations, 3) the hydrostatic and 5) the nonhydrostatic inertia–gravity wave simulations, 4) the fully compressible hydrostatic and 8) nonhydrostatic mountain wave simulations, and 6) the Boussinesq hydrostatic and 7) nonhydrostatic mountain wave simulations.

scaled divergences collapse roughly onto the same curve. Equation (29) was arrived at by our observation that $\epsilon \sim \Delta t$ rms [div ($\mathbf{V}$)], and that rms [div ($\mathbf{V}$)] $\sim \delta u'/\Delta x$. Thus, a reasonable estimate of u' or the rms [div($\mathbf{V}$)] is all that is needed to determine ϵ_c prior to a simulation.

5. Summary

We have demonstrated that compressible nonhydrostatic semi-implicit numerical models can be efficiently integrated using preconditioned conjugate-residual solvers. The CR algorithm, along with appropriate preconditioners, accurately and efficiently solve the Helmholtz equations arising from the semi-implicit discretization for modeling applications ranging from hydrostatic to nonhydrostatic scales. Moreover, the flexibility of the CR solvers allow the solution of general Helmholtz equations with variable coefficients and cross-derivative terms included. Thus, the inclusion of a reference state into the model formulation for the purpose of regularizing the Helmholtz equation, as well as the explicit integration of the terrain terms and so-called nonlinear pressure gradient and divergence terms, are not needed, and need not dictate the model formulation. We propose and demonstrate a more consistent and straightforward model formulation that includes the full pressure gradient and divergence terms in the semi-implicit formulation, along with terms responsible for buoyancy oscillations. This formulation should provide greater accuracy and stability, particularly in nonhydrostatic scale

simulations involving steep terrain where the traditional formulation is unstable.

Two variants of an ADI preconditioner are used in the CR algorithm. First, for hydrostatic flows (typically using $\Delta x \geq 5$–10 km) a single vertical sweep of the ADI method is a very effective preconditioner. The ADI parameter β_2 in (28b) should be large, $O(50) \rightarrow O(500)$. A single sweep of the full ADI method (28) should be used for nonhydrostatic flows, and the parameters β_1 and β_2 should be $O(10)$ or less. We have not found it necessary to include the terrain terms in the ADI formulation in our test cases, thus the ADI preconditioner and the CR algorithm are easily implemented.

The CR algorithm need not be iterated until convergence to machine accuracy. We find that further reduction of the residual in the Helmholtz solution, after convergence to a particular level, does not increase the accuracy of the overall solution. An a priori estimate of the maximum allowable residual (ϵ_c) necessary for accurate solutions in the semi-implicit models, for all simulation scales, is given in (29). Here, ϵ_c is found to depend on the rms divergence in the solution, which can be estimated from the time step, grid-length, and velocity scales in the simulations.

The number of CR iterations needed for convergence to ϵ_c is roughly proportional to the time step for most of the flows we have simulated, even when a preconditioner is used. Thus, given that the semi-implicit time step in forward-in-time models is effectively one-half that of leapfrog models, the semi-implicit forward-in-time models are potentially twice as efficient as their leapfrog counterpart, all other elements remaining equal.

The CR method also can be used in semi-implicit hydrostatic models. The effectiveness of an ADI preconditioner would need to be evaluated in the hydrostatic applications. A conjugate gradient scheme with a 1D (in z) preconditioner has been used by Hill and Marshall (1995) for inverting a Poisson equation arising in an incompressible nonhydrostatic ocean model. The preconditioner is not ADI, but rather is a hydrostatic preconditioner in that it is exact in the limit of hydrostatic flow. As noted earlier, a variety of efficient preconditioners are possible and we make use of one that is easily generalized and efficient for a range of problems.

REFERENCES

Axelsson, O., 1994: *Iterative Solution Methods.* Cambridge University Press, 654 pp.

Bernadet, P., 1995: The pressure term in the anelastic model: A symmetric elliptic solver for an Arakawa C grid in generalized coordinates. *Mon. Wea. Rev.,* **123,** 2474–2490.

Coté, J. C., S. Gravel, and A. Staniforth, 1995: A generalized family of schemes that eliminate spurious resonant response of semi-Lagrangian schemes to orographic forcing. *Mon. Wea. Rev.,* **123,** 3605–3613.

Cullen, M. J. P., 1990: A test of a semi-implicit integration technique for a fully compressible non-hydrostatic model. *Quart. J. Roy. Meteor. Soc.,* **116,** 1253–1258.

——, and J. James, 1994: A comparison of two different vertical grid staggerings. *Proc. 10th Conf. on Numerical Weather Prediction,* Portland, OR, Amer. Meteor. Soc., 38–40.

Douglas, J., 1962: Alternating direction methods for three space variables, *Numerische Mathematik,* **4,** 41–63.

Durran, D. R., and J. B. Klemp, 1983: A compressible model for the simulation of moist mountain waves. *Mon. Wea. Rev.,* **111,** 2341–2361.

Eisenstat, S. C., H. C. Elman, and M. H. Schultz, 1983: Variational iterative methods for nonsymmetric systems of linear equations. *SIAM J. Numer. Anal.,* **20,** 345–357.

Gal-Chen, T., and R. J. C. Somerville, 1975: On the use of a coordinate transformation for the solution to the Navier–Stokes equations. *J. Comput. Phys.,* **17,** 209–228.

Golding, B. W., 1992: An efficient non-hydrostatic forecast model. *Meteor. Atmos. Phys.,* **50,** 89–103.

Hestenes, M. R., and E. Stiefel, 1952: Methods of conjugate gradients for solving linear systems. *J. Res. Natl. Bur. Stand.,* **49,** 409–436.

Hill, C., and J. Marshall, 1995: Application of a parallel Navier–Stokes model to ocean circulation. *Parallel Computational Fluid Dynamics.,* A. Ecer, J. Periaux, N. Satofuka, and S. Taylor, Eds., Elsevier, 545–552.

Ikawa, M., 1988: Comparison of some schemes for nonhydrostatic models with orography. *J. Meteor. Soc. Japan,* **66,** 753–776.

Kapitza, H., and D. Eppel, 1992: The non-hydrostatic mesoscale model GESIMA. Part 1: Dynamical equations and tests. *Beitr. Phys. Atmos.,* **65,** 129–146.

Klemp, J. B., and R. Wilhelmson, 1978: The simulation of three-dimensional convective storm dynamics. *J. Atmos. Sci.,* **35,** 1070–1096.

Roache, P. J., 1972: *Computational Fluid Dynamics.* Hermosa Publishers, 446 pp.

Rotunno, R., W. C. Skamarock, and C. Snyder, 1994: An analysis of frontogenesis in numerical simulations of baroclinic waves. *J. Atmos. Sci.,* **51,** 3373–3398.

Semazzi, F. H. M., J. H. Qian, and J. S. Scroggs, 1995: A global nonhydrostatic semi-Lagrangian atmospheric model without orography. *Mon. Wea. Rev.,* **123,** 2534–2550.

Skamarock, W. C., and J. B. Klemp, 1992: The stability of time-split numerical methods for the hydrostatic and nonhydrostatic elastic equations. *Mon. Wea. Rev.,* **120,** 2109–2127.

——, and ——, 1993: Adaptive grid refinement for two-dimensional and three-dimensional nonhydrostatic atmospheric flow. *Mon. Wea. Rev.,* **121,** 788–804.

——, and ——, 1994: Efficiency and accuracy of the Klemp–Wilhelmson time-splitting technique. *Mon. Wea. Rev.,* **122,** 2623–2630.

Smolarkiewicz, P. K., and L. G. Margolin, 1994: Variational solver for elliptic problems in atmospheric flows. *Appl. Math. Comp. Sci.,* **4,** 527–551.

——, V. Grubišić, and L. G. Margolin, 1997: On forward-in-time differencing for fluids: Stopping criteria for iterative solutions of anelastic pressure equations. *Mon. Wea. Rev.,* **125,** 647–654.

Stiefel, E. L., 1955: Relaxationsmethoden bester Strategie zur losung linearer Gleichungssystems. *Comment. Math. Helv.,* **29,** 157–179.

Stoer, J., 1983: Solution of large linear systems of equations by conjugate gradient type methods. *Mathematical Programming: The State of the Art,* A. Bachem, M. Grotschel, and B. Korte, Eds., Springer-Verlag, 655 pp.

Tanguay, M., A. Robert, and R. Laprise, 1990: A semi-implicit semi-Lagrangian fully compressible regional forecast model. *Mon. Wea. Rev.,* **118,** 1970–1980.